JACS
JOURNAL OF THE AMERICAN CHEMICAL SOCIETY

Communication

pubs.acs.org/JACS

Analysis of UDP-D-Apiose/UDP-D-Xylose Synthase-Catalyzed Conversion of UDP-D-Apiose Phosphonate to UDP-D-Xylose Phosphonate: Implications for a Retroaldol−Aldol Mechanism

Sei-hyun Choi, Steven O. Mansoorabadi, Yung-nan Liu, Tun-Cheng Chien, and Hung-wen Liu*

Division of Medicinal Chemistry, College of Pharmacy, and Department of Chemistry and Biochemistry, University of Texas at Austin, Austin, Texas 78712, United States

Supporting Information

ABSTRACT: UDP-D-apiose/UDP-D-xylose synthase (AXS) catalyzes the conversion of UDP-D-glucuronic acid to UDP-D-apiose and UDP-D-xylose. An acetyl-protected phosphonate analogue of UDP-D-apiose was synthesized and used in an in situ HPLC assay to demonstrate for the first time the ability of AXS to interconvert the two reaction products. Density functional theory calculations provided insight into the energetics of this process and the apparent inability of AXS to catalyze the conversion of UDP-D-xylose to UDP-D-apiose. The data suggest that this observation is unlikely to be due to an unfavorable equilibrium but rather results from substrate inhibition by the most stable chair conformation of UDP-D-xylose. The detection of xylose cyclic phosphonate as the turnover product reveals significant new details about the AXS-catalyzed reaction and supports the proposed retroaldol−aldol mechanism of catalysis.

D-Apiose (**1**) is a rare branched-chain furanose found in the cell wall of plants.[1] D-Apiose residues play an important role in plant growth and development by cross-linking cell-wall polysaccharides through the formation of a borate tetraester.[2] UDP-D-apiose (**2**), the in vivo D-apiose donor, is formed from uridine-5′-diphosphate-D-glucuronic acid (UDP-GlcA, **3**) in an unusual ring-contraction reaction catalyzed by UDP-D-apiose/UDP-D-xylose synthase (AXS). The conversion of **3** to **2** by AXS is NAD^+-dependent and generates UDP-D-xylose (**7**) as a side product.[3] The proposed reaction sequence for the formation of **2** (Scheme 1) involves oxidative decarboxylation of **3** to afford a 4-ketoxylose intermediate (UDP-4-KX, **4**). Subsequent ring contraction (**4** → **6**) followed by reduction at C3′ by NADH yields **2**.

Two plausible mechanisms for the ring-contraction step have been proposed.[4] In the first mechanism (Scheme 1, pathway A), the C2−C3 bond of **4** is cleaved in a retroaldol reaction, yielding an enediol intermediate (**5**) that cyclizes in an aldol reaction to give **6**. In the second mechanism (Scheme 1, pathway B), **6** is formed from **4** directly through a 1,2-shift. In contrast to the stepwise retroaldol−aldol route, the C−C bond migration in this concerted mechanism would bypass the formation of a discrete intermediate such as **5**. In both mechanisms, the formation of **7** could result from a premature reduction of the decarboxylated 4-keto intermediate **4** by NADH prior to the rearrangement step.

Scheme 1. Proposed Mechanisms for the AXS-Catalyzed Biosynthesis of UDP-D-apiose (2) and UDP-D-xylose (7) from UDP-GlcA (3)

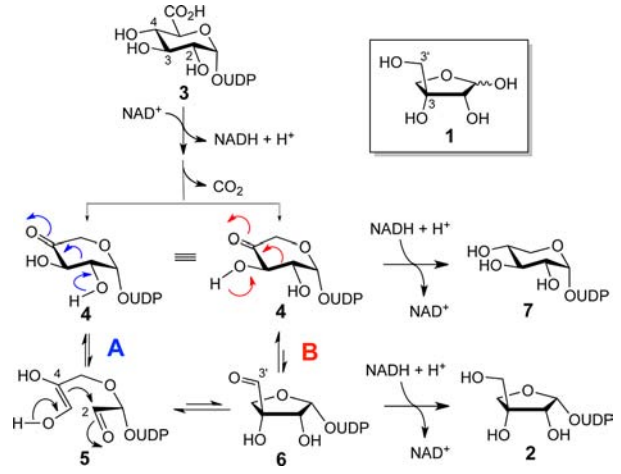

One curious observation from previous studies is that AXS is unable to convert **7** to **2**,[5] suggesting that there is no mechanistic link between these two products and that each is formed irreversibly.[5c] However, testing this hypothesis is challenging because of the instability of **2** in aqueous solution,[6] which makes direct detection of its formation in vitro difficult. One potential strategy to circumvent this issue and gain insight into the mechanism of the AXS-catalyzed ring contraction may be to assay the reaction in the energetically favorable reverse direction (**2** → **7**) using a stable UDP-D-apiose analogue as the substrate. Accordingly, we designed and synthesized **8**, a phosphonate analogue of **2** (Figure 1), and examined its interaction with AXS. Compound **8** was chosen because phosphonates are well-established as stable analogues of

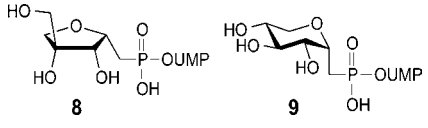

Figure 1. Phosphonate analogues of UDP-D-apiose (**8**) and UDP-xylose (**9**).

Received: June 7, 2012
Published: July 25, 2012

dx.doi.org/10.1021/ja305322x | J. Am. Chem. Soc. 2012, 134, 13946−13949

phosphates.[7] In addition, density functional theory (DFT) calculations provided insight into the energetics of the AXS-catalyzed reaction. The results are described herein.

Because of the tertiary carbon center at C3, the key step in the synthesis of D-apiose analogues is the introduction of the hydroxymethyl moiety. Several synthetic strategies were attempted to introduce the C3-methyl branch in the synthesis of D-apiose analogue **8** (Scheme 2). Starting from isopropylidene-protected xylofuranose (**11**), sequential protection of the free hydroxyl groups gave protected xylose **12**. Deprotection of the isopropylidene group, reduction of the anomeric carbon,[8] and oxidation of the 3-hydroxyl moiety afforded 3-keto-4-deoxysugar **14**. For the introduction of the hydroxymethyl moiety at C3, a Wittig reaction followed by a dihydroxylation protocol was attempted. However, careful NMR assignment [Figure S1A in the Supporting Information (SI)] and X-ray crystallographic analysis (Figure 2A) revealed that the stereochemistry of the product at C3 was opposite that of the desired product. This result can be rationalized by considering that osmium tetroxide would approach from the less sterically hindered *Si* face during the hydroxylation step (Figure 2B).

Scheme 2. Attempts To Synthesize 8

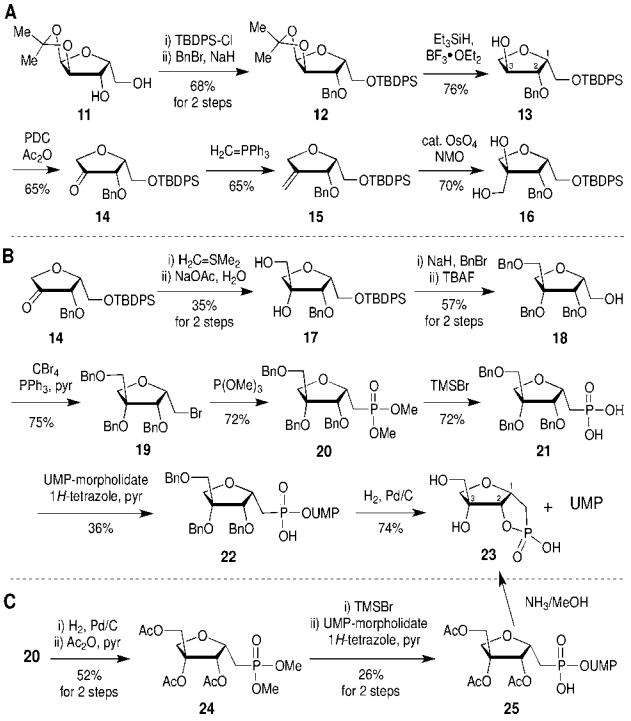

The introduction of the hydroxymethyl group with the desired configuration was then attempted using ylide chemistry (Scheme 2B). As with OsO_4, a sulfur ylide would be expected to attack from the *Si* face. The nuclear Overhauser effect spectroscopy (NOESY) NMR spectrum of the hydrolyzed product **17** revealed that it contained the desired configuration (Figure S1B). Consecutive protection of the hydroxyls with benzyl groups, deprotection of the TBDPS group, bromination with CBr_4, and phosphonylation afforded protected apiose phosphonate analogue **20**. Hydrolysis of the methyl phosphonate to the corresponding phosphonic acid (**21**) and coupling with uridine-5′-monophosphate (UMP) morpholidate afforded **22**, a benzyl-protected UMP phosphonate analogue of D-apiose.[9] However, after deprotection of the benzyl groups, cyclic phosphonate **23** was obtained.

With the hope that this intramolecular cyclization problem could be overcome under mildly basic conditions, a tri-*O*-acetyl-protected UMP phosphonate analogue of D-apiose, **25**, was synthesized (Scheme 2C). However, even under mild conditions (0.2 M NH_3 in MeOH, 0 °C), **23** and UMP were the only products obtained. A possible explanation for these results is that the 2-alkoxide ion formed during the reaction is suitably aligned to attack the vicinal phosphorus center, forming the thermodynamically stable five-membered cyclic phosphonate with concomitant release of UMP, which is a good leaving group.

In addition to the phosphonate analogue of D-apiose, we also attempted to synthesize **9**, a UMP phosphonate analogue of D-xylose, for use as a product standard (Scheme 3). The reducing end of benzyl-protected D-xylose **27** was converted into linear alkene **28** by a Wittig reaction and subsequently transformed into iodomethyl compound **29** by a successive oxymercuration−iodination reaction.[10] Only the α-isomer of **29** was isolated, possibly because of an anomeric effect. With a method similar to that applied for the synthesis of **22**, we obtained **32**, the benzyl-protected UMP phosphonate analogue of D-xylose. Hydrogenation to remove the benzyl groups also afforded cyclic phosphonate **10** and UMP as the only products.

Scheme 3. Synthesis of Xylose Cyclic Phosphonate 10

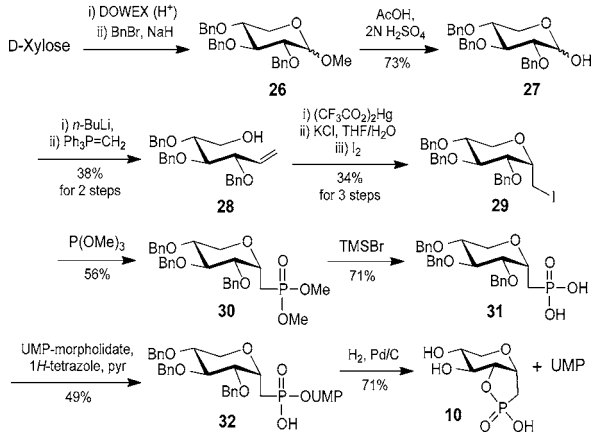

Although phosphonates are known to be more stable than the corresponding phosphates in terms of their anomeric bond strength, these results suggest that the P−OUMP bond of the phosphonate analogues can still be readily cleaved when the 2-

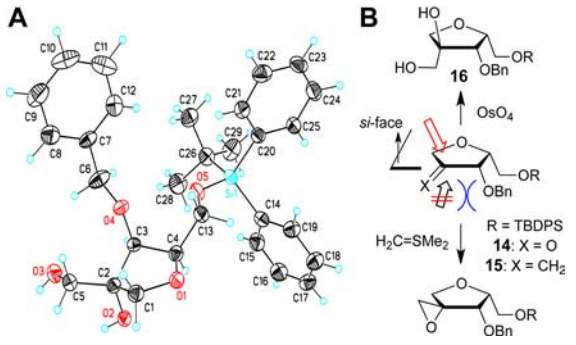

Figure 2. (A) X-ray structure of **16**. (B) Explanation of the observed stereochemistry of the methylenation of **14** and dihydroxylation of **15**.

dx.doi.org/10.1021/ja305322x | J. Am. Chem. Soc. 2012, 134, 13946−13949

OH group is well-aligned for nucleophilic attack. One potential way to overcome the intrinsic instability of **8** would be to generate it in situ during the assay of AXS activity. A coupled assay using an acetyl esterase and AXS was therefore designed in which **8** would be generated from acetyl-protected substrate **25**. Orange peel acetyl esterase (AE, E.C. 3.1.1.6) was chosen because it is known to deacetylate various peracetylated NDP sugars in good yield.[11] **25** was incubated with AE for 24 h, and mass spectrometry (MS) analysis showed that it was deacetylated to give the desired product, **8** (see the SI).

Having established that **8** could be synthesized enzymatically from **25** using AE, an in situ HPLC assay of AXS activity was attempted using dual UV−vis and Corona-charged aerosol detection.[12] The latter is able to visualize nonvolatile compounds regardless of whether they have a chromophore. The Corona HPLC traces of the AXS reaction mixtures (Figure 3a,b) contain a broad peak between 11 and 13 min.

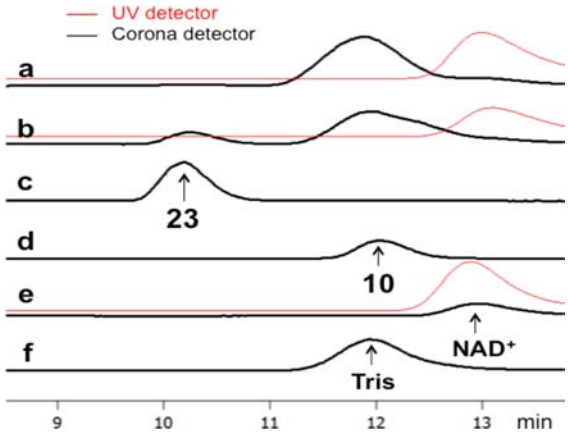

Figure 3. HPLC traces for the in situ AXS assay with dual detection (black line, Corona detector; red line, UV detector): (a) reaction mixture at 0 h; (b) reaction mixture at 47 h; (c) apiose cyclic phosphonate **23**; (d) xylose cyclic phosphonate **10**; (e) NAD^+; (f) Tris.

Comparison with the HPLC traces of the individual reaction components showed that NAD^+ (Figure 3e) and Tris buffer (Figure 3f) both elute in this region. Xylose cyclic phosphonate **10**, the product of the attempted synthesis of **9**, also elutes within this region (Figure 3d). After a 47 h reaction period, a new peak with a retention time of 10 min was observed, consistent with the formation of a small amount of apiose cylic phosphonate **23** (Figure 3b,c). In addition, a shoulder appeared to form on the broad peak centered at ∼12 min.

To verify that this shoulder indicates the formation of **10**, and thus the conversion of **8** to **9** by AXS, the peak between 11 and 12.5 min was collected and analyzed by MS. The MS data are indeed consistent with the peak containing both **10** ($[M - H]^-$, m/z 209) and Tris ($[M + H]^+$, m/z 122) (see the SI). To ensure that the species detected by MS corresponded to xylose cyclic phosphonate **10** and not contaminating apiose cyclic phosphonate **23**, the isolated peak was fractionated using diethylaminoethyl (DEAE) resin ion-exchange chromatography, and each fraction was reanalyzed by HPLC. As shown in Figure 4, Tris (11 min) eluted in the H_2O wash fractions (f1 and f2), whereas **10** (12 min) eluted at high ammonium bicarbonate concentrations (f14−f18). There was no evidence for the presence of **23** (10 min) in any of the fractions. These results clearly show that the broad peak indeed contains **10**,

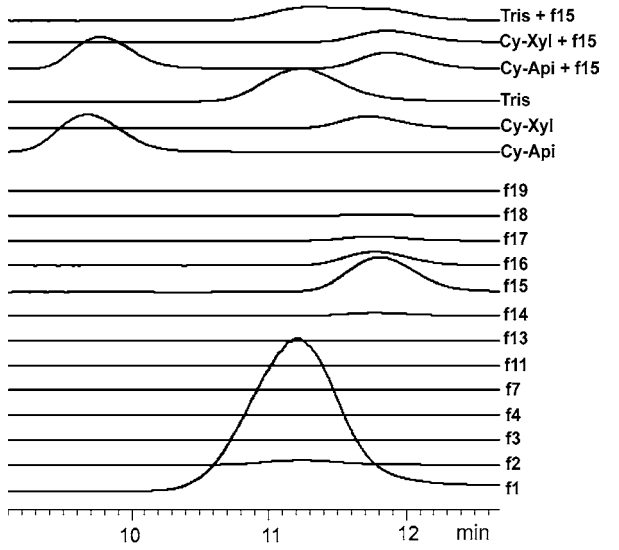

Figure 4. HPLC traces of the isolated 11−12.5 min peak using DEAE resin ion-exchange chromatography. For detailed experimental procedures, see the SI.

indicating that AXS can catalyze the conversion of UDP-D-apiose analogue **8** to the corresponding UDP-D-xylose analogue **9**, which degrades into **10**.

The observation that AXS can catalyze the reverse reaction, the conversion of **8** to **9**, contrasts with the previous result that **7** could not be converted to **2** by AXS.[5] To gain insight into these different reactivities, the energetics of the reaction was examined by DFT calculations using Gaussian 98.[13] The calculations (performed at the B3LYP/6-311+G(d,p) level using a scaling factor of 0.9877 and the polarizable continuum model to mimic solvent) showed that in aqueous solution, the chair conformation of D-xylose with the hydroxyl groups in the equatorial position (e.g., **7**) is only 0.4 kcal/mol more stable than D-apiose (e.g., **2**). Such a small difference in free energy is unable to account for the apparent inability of AXS to convert **7** to **2**. Surprisingly, however, it was found that the alternative chair conformation of D-xylose in which the hydroxyl groups are in the axial position (e.g., **33**) is 1.6 kcal/mol more stable than D-apiose.

The less stable D-xylose conformer, **7**, would be expected to bind to AXS in a manner analogous to the substrate, **3**, with the 4-H properly oriented for transfer to NAD^+ (Scheme 4). In contrast, the more stable D-xylose conformer, **33**, overlays quite well with the product, **2** (Scheme 4 inset). In this binding mode, the catalytic base required for the oxidation of the hydroxymethyl moiety of **2** would interact with the C3 hydroxyl instead of the C4 hydroxyl of **33**. Thus, **33** would not be positioned for efficient hydride transfer to NAD^+, and its binding to AXS would result in the formation of a dead-end complex. The combined observations give a possible explanation for the apparent inability of AXS to catalyze the conversion of **7** to **2**: the former can adopt two conformations in solution, the more stable of which inhibits the enzyme. This inhibition may have prevented the detection of **2** under the conditions and time scale used in the previous studies.[5]

The detection of xylose cyclic phosphonate **10** instead of **9** as the product of the incubation of **8** with AXS is another significant finding. Since compound **10** must be derived from **9** via nucleophilic attack at the vicinal phosphorus center by the 2-alkoxide anion, the above observation strongly suggests that

dx.doi.org/10.1021/ja305322x | J. Am. Chem. Soc. 2012, 134, 13946−13949

Scheme 4. Energy Differences between the Two Conformers of UDP-D-xylose[a]

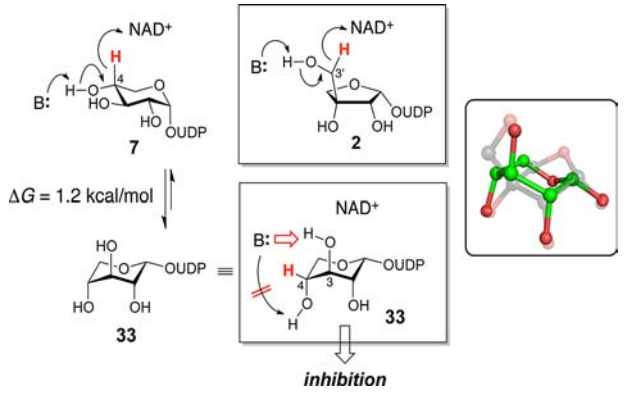

[a]The less stable conformer, **7**, can bind productively and be converted to UDP-D-apiose, while the more stable conformation, **33**, forms a dead-end complex. The inset shows an overlay of **33** (green) and **2** (gray).

deprotonation of the 2-OH group occurs during the conversion of **2** to **7**. Of the two mechanisms proposed for AXS, only the cleavage of the C2−C3 bond of **4** in a retroaldol process requires the ionization of the 2-OH group (**4** → **5**; Scheme 1, pathway A). In contrast, the 1,2-shift mechanism (Scheme 1, pathway B) requires deprotonation of the C3 hydroxyl group (**4** → **6**). Taken together, the current data support the stepwise retroaldol−aldol route as the catalytic mechanism of AXS.

In summary, we synthesized **8**, a protected phosphonate analogue of UDP-D-apiose (**2**), for use in mechanistic studies of AXS. To overcome the intrinsic instability of **8** during chemical synthesis, a coupled assay in which this substrate was generated in situ using acetyl esterase was developed. The data show that AXS can accept phosphonate in addition to the natural phosphate substrates. More importantly, our results reveal that AXS converts **8** into the corresponding UDP-D-xylose analogue **9**, which is inconsistent with the assertion that there is no mechanistic link between the biosyntheses of the two products **2** and **7** formed by the AXS-catalyzed reaction with UDP-GlcA (**3**).[5c] Insight into the apparent inability of AXS to convert **7** to **2** was obtained from DFT calculations, which suggested that this observation is unlikely to arise from the endergonicity of the reaction. Instead, it was found that **7** can exist in two stable chair conformations in aqueous solution, the more favorable of which is likely to bind unproductively to AXS and inhibit its activity. This product inhibition of the AXS-catalyzed reaction by UDP-D-xylose may play a physiological role in the regulation of cell-wall biogenesis in plants. Moreover, the isolation of **10** instead of **9** as the turnover product of **8** with AXS provides strong evidence in support of the retroaldol−aldol mechanism for this intriguing enzyme.

■ ASSOCIATED CONTENT

Supporting Information

Materials and methods and spectroscopic and structural data. This material is available free of charge via the Internet at http://pubs.acs.org.

■ AUTHOR INFORMATION

Corresponding Author

h.w.liu@mail.utexas.edu

Notes

The authors declare no competing financial interest.

■ ACKNOWLEDGMENTS

We thank Dr. Mikio Fuji for his contributions to the initial synthetic efforts. This work was supported by grants from the National Institutes of Health (GM035906 and GM054346) and the Welch Foundation (F-1511).

■ REFERENCES

(1) (a) Ishii, T.; Matsunaga, T.; Pellerin, P.; O'Neill, M. A.; Darvill, A.; Albersheim, P. *J. Biol. Chem.* **1999**, *274*, 13098. (b) O'Neill, M. A.; Ishii, T.; Albersheim, P.; Darvill, A. G. *Annu. Rev. Plant Biol.* **2004**, *55*, 109. (c) Beck, E. *Z. Pflanzenphysiol.* **1967**, *57*, 444. (d) Longland, J. M.; Fry, S. C.; Trewavas, A. J. *Plant Physiol.* **1989**, *90*, 972.

(2) O'Neill, M. A.; Eberhard, S.; Albersheim, P.; Darvill, A. G. *Science* **2001**, *294*, 846.

(3) (a) Picken, J. M.; Mendicino, J. *J. Biol. Chem.* **1967**, *242*, 1629. (b) Mendicino, J. *Biochim. Biophys. Acta* **1974**, *364*, 159. (c) Pan, Y. T.; Kindel, P. K. *Arch. Biochem. Biophys.* **1977**, *181*, 131.

(4) Choi, S.-h.; Ruszczycky, M. W.; Zhang, H.; Liu, H.-w. *Chem. Commun.* **2011**, *47*, 10130.

(5) (a) Baron, D.; Wellmann, E.; Grisebach, F. *Biochim. Biophys. Acta* **1972**, *258*, 310. (b) Baron, D.; Grisebach, F. *Eur. J. Biochem.* **1973**, *38*, 153. (c) Mølhøj, M.; Verma, R.; Reiter, W. D. *Plant J.* **2003**, *35*, 693.

(6) (a) Kindel, P. K.; Watson, R. R. *Biochem. J.* **1973**, *133*, 277. (b) Guyett, P.; Glushka, J.; Gu, X.; Bar-Peled, M. *Carbohydr. Res.* **2009**, *344*, 1072.

(7) (a) Du, Y.; Linhardt, R. J. *Tetrahedron* **1998**, *54*, 9913. (b) Uchiyama, T.; Vassilev, V. P.; Kajimoto, T.; Wong, W.; Huang, H.; Lin, C.-c.; Wong, C.-H. *J. Am. Chem. Soc.* **1995**, *117*, 5395. (c) Compain, P.; Martin, O. R. *Bioorg. Med. Chem.* **2001**, *9*, 3077. (d) Zhao, Z.; Hong, L.; Liu, H.-w. *J. Am. Chem. Soc.* **2005**, *127*, 7692.

(8) Ewing, G. J.; Robins, M. J. *Org. Lett.* **1999**, *1*, 635.

(9) Wittmann, V.; Wong, C.-H. *J. Org. Chem.* **1997**, *62*, 2144.

(10) Garneau, S.; Qiao, L.; Chen, L.; Walker, S.; Vederas, J. C. *Bioorg. Med. Chem.* **2004**, *12*, 6473.

(11) (a) Baisch, G.; Ohrlein, R. *Bioorg. Med. Chem.* **1997**, *5*, 383. (b) Waldmann, H.; Heuser, A. *Bioorg. Med. Chem.* **1994**, *2*, 477.

(12) Tris buffer (11.8 mM) was used in the assay even though it coelutes with **10** under the HPLC conditions used (14 mM NH_4OAc, isocratic elution) because AXS showed the best activity in this buffer (e.g., no AXS activity could be detected in phosphate buffer).

(13) Frisch, M. J.; Trucks, G. W.; Schlegel, H. B.; Scuseria, G. E.; Robb, M. A.; Cheeseman, J. R.; Zakrzewski, V. G.; Montgomery, J. A., Jr.; Stratmann, R. E.; Burant, J. C.; Dapprich, S.; Millam, J. M.; Daniels, A. D.; Kudin, K. N.; Strain, M. C.; Farkas, O.; Tomasi, J.; Barone, V.; Cossi, M.; Cammi, R.; Mennucci, B.; Pomelli, C.; Adamo, C.; Clifford, S.; Ochterski, J.; Petersson, G. A.; Ayala, P. Y.; Cui, Q.; Morokuma, K.; Malick, D. K.; Rabuck, A. D.; Raghavachari, K.; Foresman, J. B.; Cioslowski, J.; Ortiz, J. V.; Baboul, A. G.; Stefanov, B. B.; Liu, G.; Liashenko, A.; Piskorz, P.; Komaromi, I.; Gomperts, R.; Martin, R. L.; Fox, D. J.; Keith, T.; Al-Laham, M. A.; Peng, C. Y.; Nanayakkara, A.; Gonzalez, C.; Challacombe, M.; Gill, P. M. W.; Johnson, B.; Chen, W.; Wong, M. W.; Andres, J. L.; Head-Gordon, M.; Replogle, E. S.; Pople, J. A. *Gaussian 98*, revision A.9; Gaussian, Inc.: Pittsburgh, PA, 1998.